

RESEARCH ARTICLE

Catalytic desorption of CO₂-loaded solutions of diethylethanolamine using bentonite catalyst

Urvashi K. Sarode | Prakash D. Vaidya 

Department of Chemical Engineering,
Institute of Chemical Technology,
Nathalal Parekh Marg, Mumbai, India

Correspondence

Prakash D. Vaidya, Department of
Chemical Engineering, Institute of
Chemical Technology, Nathalal Parekh
Marg, Matunga, Mumbai-400019, India.
Email: pd.vaidya@ictmumbai.edu.in

Funding information

Department of Science and Technology,
Ministry of Science and Technology,
Government of India, New Delhi,
Grant/Award Number: DST/TM/EWO/
MI/CCUS/11(G) dated September 2019

Abstract

The absorption of CO₂ gas into aqueous alkanolamine solutions is the most advanced CO₂ separation technology and a key challenge in this technique is the energy-intensive process of solvent regeneration. The tertiary amine *N,N'*-diethylethanolamine (or DEEA) is a candidate CO₂-capturing solvent with potential. To improve the energy efficiency of regeneration of DEEA, several catalysts were used for desorbing CO₂ from loaded solutions of DEEA (2.5 M) at $T = 363$ K. Desorption trials were conducted in batch mode. The initial CO₂ loading varied in the 0.3–0.35 mol CO₂/mol DEEA range. The performance was analyzed by calculating the rate of CO₂ desorption, cyclic capacity, and reduction in sensible energy. The amount of thermal energy needed for amine regeneration was significantly lowered by using nine transition metal oxide catalysts and the hierarchy was as follows: Al₂O₃ < MoO₃ < V₂O₅ < TiO₂ < MnO₂ < ZnO < Cr₂O₃ < SiO₂ < ZrO₂. Among the metal oxides, Al₂O₃ increased desorption efficiency compared to blank runs by 89%. A clay-based powder bentonite was also used as catalyst and its efficacy was compared with the metal oxides. This cheap and easily available bentonite catalyst was tuned through simple ion-exchange with four acids (HCl, H₃PO₄, HNO₃, and H₂SO₄). Upon treatment with H₂SO₄, bentonite remarkably increased desorption efficiency by 100%. Furthermore, bentonite catalyst treated with sulphuric acid (denoted here as Bt/H₂SO₄) was characterized by Brunauer–Emmett–Teller (BET), scanning electron microscopy (SEM), Fourier transform infrared spectrometry (FTIR), X-ray diffraction (XRD), and ammonia temperature-programmed desorption (NH₃-TPD). In this way, a comprehensive study on catalytic desorption of DEEA was performed.

KEYWORDS

alkanolamine, bentonite, carbon dioxide, catalyst, desorption

1 | INTRODUCTION

CO₂ gas absorption in one or more basic absorbents, such as aqueous solutions of primary, secondary, and tertiary alkanolamines, is widely used for the separation of CO₂ from industrial gases.^[1] A good feature of the reactive

absorption process is that the solvent can be regenerated by raising the temperature in the desorption column.^[2] The most popular primary amine monoethanolamine (MEA) and the secondary amine diethanolamine (DEA) exhibit some advantages like high absorption kinetics and low solvent cost. However, they also suffer from

several drawbacks, such as a high heat energy requirement for solvent regeneration, equipment corrosion, solvent degradation, and low CO₂ cyclic capacity (0.5 mol CO₂/mol amine). Tertiary amines are high capacity solvents (1 mol CO₂/mol amine) and are easier to regenerate than primary and secondary amines.^[3] Vaidya and Kenig^[4] proposed *N,N'*-diethylethanolamine (DEEA) as a potential tertiary amine for CO₂ capture. In a past work, Sutar et al.^[5] reported data on the kinetics of CO₂ absorption and equilibrium CO₂ solubility in aqueous DEEA and its blended solutions. Chowdhury et al.^[6] reported values of the rate of absorption, cyclic capacity, and heat of absorption for 26 tertiary amines. They found that DEEA was one among the seven absorbents which exhibit high absorption rate and cyclic capacity and low heat of absorption. It is thus evident that DEEA is a credible alternative.

Catalytic desorption is a candidate method for improving the amine regeneration process. Bhatti and co-workers^[7–9] extensively used various metal oxides for energy-efficient amine regeneration. For example, they showed that TiO₂, Cr₂O₃, and WO₃ reduced the sensible energy constraint of MEA (5 M) by 25%–30%, while V₂O₅ and MoO₃ achieved 44%–48% reduction.^[7] In another work, it was proven that ZrO₂ and ZnO improved the regeneration of CO₂-rich MEA.^[8] For instance, both oxides desorbed more CO₂ (up to 32%), improved CO₂ desorption rate (up to 54%), and increased cyclic loading (up to 56%). Moreover, five new metal oxides were applied for loaded solutions of MEA: Ag₂O, Nb₂O₅, NiO, CuO, and MnO₂.^[9] Both Ag₂O and Nb₂O₅ exhibited the most promising performance by desorbing up to 3.6 and 2.5 times more CO₂ with faster desorption rates.

Zhang et al.^[10] used Fe-promoted sulphated zirconia supported on MCM-41 catalysts (SZMF) for regenerating loaded MEA solutions at 371 K. They found that this catalyst improved desorption factor (260%–388%) and decreased heat duty (28%–40%). They attributed this superior catalytic activity to a higher ratio of Bronsted to Lewis acid sites, weakly acidic sites, basic sites, and greater dispersion of Fe³⁺ species. They also reported that SZMF exhibited high cyclic stability. In another work, promoter Fe outperformed Al and Mo, and Fe₂O₃ modified MCM-41 was shown as a superior catalyst.^[11] They proposed a dual-site pathway for the catalytic regeneration of amines over metal-promoted MCM-41 catalysts. Zhang et al.^[12] modified mesoporous molecular sieves (KIT-6) with transition metal oxides CuO, NiO, and Fe₂O₃. They found that CuO-KIT-6 catalyst was superior, possibly due to its high Bronsted acid sites and large mesoporous surface area. This catalyst retained its activity even after five absorption-desorption cycles. Tan et al.^[13] worked with cheap and eco-friendly clay catalysts, viz. attapulgite (ATP), activated bentonite (K-10),

and sepiolite (SEP). Clays are renowned for their hydrothermal stability, high surface area, and the presence of both Bronsted and Lewis acid sites. Due to these properties, they are attractive solid acid catalysts for amine regeneration. Especially, the layered silicate clay bentonite comprises montmorillonite. While all the three clays accelerated desorption of rich MEA, ATP was especially promising due to its higher rate of CO₂ desorption (54%–57%) and lower relative heat duty (32%).^[13] It was suggested that ATP performed well due to its favourable surface area and medium active sites. In a further work, Tan et al.^[14] showed that ATP modified with SnO₂ worked better than ATP or SnO₂ for regenerating MEA at 361 K. Due to its improved Bronsted acid sites and strong acid sites, this catalyst could reduce the relative heat duty by 52%. It could be recycled 12 times. It is thus possible to advance cheaper CO₂ separation using such efficient catalysts.

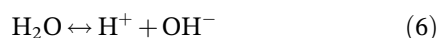
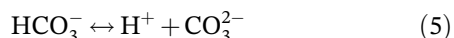
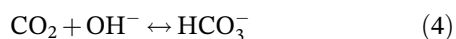
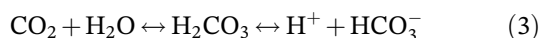
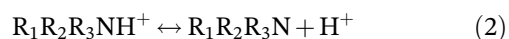
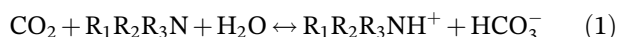
The present study is aimed at proposing remarkably good catalysts for improved regeneration of DEEA. Besides the transition metal oxides, a type of abundant clay ore bentonite was introduced as catalyst for the CO₂ desorption process. According to Grim and Guven,^[15] bentonite is a crystalline clay-like mineral formed by the devitrification and the accompanying chemical alteration of a glassy igneous material, usually volcano ash. Smectites are major clay minerals in bentonites which consist of montmorillonite, beidellite, saponite, nontro-nite, and hectonite.^[16] Smectites is the name given to a group of sodium, calcium, magnesium, iron, lithium, and aluminum silicates and the rocks in which these smectite minerals are dominant are bentonite.^[17] The industrial uses of bentonite powders depend on the quantity and quality of their smectites and other minerals. The usage also depends on the valence, type, and number of cations exchanged.^[18] In this regard, clay materials like bentonite are of particular interest because they are naturally occurring, inexpensive, and widely accessible in comparison to transition metal oxides, and are probably the most promising materials due to their high aluminosilicate content.^[19]

In this study, we investigated the regeneration performance of DEEA without and with catalysts. Here, two types of catalysts were used: (1) transition metal oxides (Al₂O₃, MoO₃, V₂O₅, TiO₂, MnO₂, ZnO, Cr₂O₃, SiO₂, and ZrO₂), and (2) clay-based powder (bentonite). Moreover, bentonite powder was separately treated with four acids (HCl, H₃PO₄, HNO₃, and H₂SO₄) to improve the active acidic sites, which eventually increased the CO₂ desorption rate of the amine solvent. The solute gas CO₂ was absorbed in 2.5 M DEEA solution (29.2 wt.%) until the loading was in the 0.3–0.35 mol CO₂/mol DEEA range and the solvent regeneration performance was

determined at $T = 363$ K. Most researchers used similar ranges of amine strength (~ 30 wt.%) and CO_2 loading, and thus, comparison of our outcomes with past works would be easier. The performance was analyzed by calculating the CO_2 desorption rate, cyclic capacity, amount of desorbed CO_2 , and reduction in sensible heat energy for the catalytic and non-catalytic systems. The bentonite catalyst treated with sulphuric acid ($\text{Bt}/\text{H}_2\text{SO}_4$) performed better than the other acid-treated catalysts. Further, $\text{Bt}/\text{H}_2\text{SO}_4$ was characterized using Brunauer–Emmett–Teller (BET), scanning electron microscopy (SEM), Fourier transform infrared spectrometry (FTIR), x-ray diffraction (XRD), and ammonia temperature-programmed desorption (NH_3 -TPD) to record the physiochemical modifications induced by the acid treatment. This is the first study on the regeneration of CO_2 -rich solutions of DEEA using cheaper clay materials.

2 | THEORY

Generally, in aqueous solutions of primary amines, the carbamate formation reaction is the main absorption mechanism, and bicarbonate formation occurs at high concentrations of carbamate in CO_2 -rich solvent.^[20] Therefore, during the regeneration of primary amine solutions, a considerably high amount of energy is required. However, tertiary amines can react indirectly with CO_2 molecules and produce bicarbonate instead of carbamate. Consequently, the regeneration energy required for tertiary amines is less compared to the primary amine solutions.^[21] The reaction pathway for the tertiary amine ($\text{R}_1\text{R}_2\text{R}_3\text{N}$) is given below in Equations (1)–(6).^[22] The major reaction is Equation (1). In the case of tertiary amines, the major anion is bicarbonate (HCO_3^-). In primary (R_1NH_2) and secondary amine ($\text{R}_1\text{R}_2\text{NH}$), the major anion is carbamate ($\text{R}_1\text{R}_2\text{N} - \text{COO}^-$).



The zwitterion mechanism^[23,24] and termolecular mechanism are suitable for CO_2 reactions with primary

and secondary amines.^[25] The tertiary amine ($\text{R}_1\text{R}_2\text{R}_3\text{N}$) does not react directly with CO_2 ; these amines have a base-catalytic effect on the hydration of CO_2 based on Equation (1).^[26] Equation (7) denotes the rate equation for the tertiary amine (R_3N)^[27]:

$$r_{\text{CO}_2} = k_{\text{R}_3\text{N}}(\text{R}_3\text{N})(\text{CO}_2) \quad (7)$$

3 | EXPERIMENTAL SECTION

3.1 | Materials

DEEA, (purity 99%), methanol (purity 99%), sodium hydroxide flakes (NaOH , purity 97%), and all metal oxides Al_2O_3 , V_2O_5 , MnO_2 , ZnO , Cr_2O_3 , ZrO_2 , TiO_2 , SiO_2 , and MoO_3 were purchased from Molychem Chemicals, Mumbai. The natural clay mineral bentonite powder (aluminum silicate hydrate) and the activating agents used in acid treatment such as hydrochloric acid (HCl , 36.46%), phosphoric acid (H_3PO_4 , 98%), sulphuric acid (H_2SO_4 , 98%), and nitric acid (HNO_3 , 72%) were also supplied by Molychem Chemicals, Mumbai. Cylinders containing carbon dioxide (CO_2) and nitrogen (N_2) were bought from Inox Air Products Ltd., Mumbai (gas purity 99.95%).

3.2 | Experimental apparatus and procedure

A stirred-tank reactor was used for CO_2 absorption in the DEEA solution (2.5 M) at 308 K. Since equilibrium CO_2 solubility reduces with temperature, a lower absorption temperature (308 K) was chosen. Upon full saturation of DEEA with CO_2 at 308 K, the rich loading was checked by using an auto-titrator (877 Titrano Plus, Metrohm) to determine the moles of CO_2 absorbed. The loading of the amine solution was maintained in the 0.3–0.35 mol CO_2 /mol DEEA range. In all experiments, 400 mL of CO_2 -loaded DEEA solution was used.

A schematic diagram of the experimental apparatus is shown in Figure 1. A four-necked flat-bottomed glass reactor inside an oil bath was used in all trials. This reactor was provided with a water-cooled condenser, stirrer, thermocouple, and sampling port. The stirrer was maintained at 200 rpm to stir the DEEA solution. The thermocouple was inserted to measure the temperature of the amine solution, while the condenser was used to condense and recycle water vapour and prevent amine loss. To study the solvent regeneration performance, 400 mL of the CO_2 -loaded DEEA solution (2.5 M) was charged inside this reactor and the oil bath was heated to

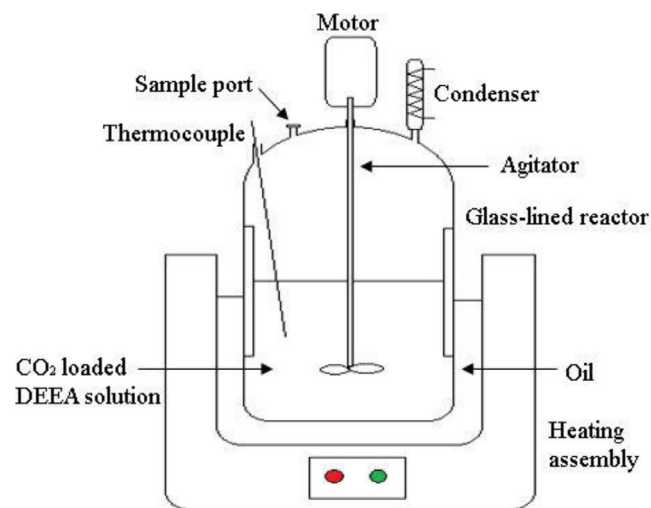


FIGURE 1 Schematic diagram of desorption setup. DEEA, *N,N*-diethylethanolamine.

maintain the reactor temperature at 363 K. The temperature was raised steadily by 283 K/min until it reached 363 K. It was observed that CO₂ loading in the amine solution changed negligibly even after 3 h at 363 K. Hence, a reaction time of 3 h was chosen. In the catalytic trials, 3 g of the respective catalyst was added to the solution in the beginning of the experiment. Upon heating, CO₂ desorption started and the values of the CO₂ loading were recorded with respect to time. The titration method from Altabash et al.^[28] and an auto-titrator were used to measure the CO₂ loadings of the solution at intervals of 0.5, 1, 1.5, 2, and 3 h. Typically, the value of pH of 50 mL methanol was adjusted to 11 by adding a solution of sodium hydroxide (NaOH). A known amount of the CO₂-loaded DEEA sample was added to methanol. The mixture was then titrated back to pH = 11 using the same NaOH solution. The volume of NaOH solution needed to maintain the pH at 11 was recorded and used to calculate the equilibrium CO₂ loading (α). The error in finding the loading values was <2%. A blank test was performed prior to all experiments and the results were used as a baseline. To validate the experimental technique, trials were performed with the benchmark solvent MEA (5 M) at $T = 363$ K. Our value of the desorption efficiency was 30%, which is in line with the value of 35% reported by Liang et al.^[29]

3.3 | Modification of the bentonite powder by acid treatment

The changes in physicochemical properties of this bentonite upon acid treatment were previously examined by Onal and Sarikaya.^[18] A sample of commercial bentonite

powder was separately treated with aqueous solutions (3 mol/L) of four acids HCl, HNO₃, H₃PO₄, and H₂SO₄ by the wet chemical method. The solid to liquid ratio was 1:15, based on dry mass of bentonite and aqueous solutions of acids.

The acid-activated bentonite samples were cooled and separated by vacuum filtration, and washed thoroughly with distilled water until the filtrate was slightly acidic (pH 5.5–6). Then, samples were dried at 373 K overnight and softly powdered.^[30] The acid-treated samples were labelled according to the acidic solution as Bt/HCl, Bt/H₃PO₄, Bt/HNO₃, and Bt/H₂SO₄ and stored in tightly closed plastic bottles.

3.4 | Data calculation

The CO₂ loading (α) is calculated by Equation (8):

$$\alpha = \frac{n_{\text{CO}_2}}{n_{\text{amine}}} \quad (8)$$

By definition, the cyclic capacity (Q_{cyc}) is the difference between the CO₂-rich loading and CO₂-lean loading.^[29]

$$Q_{\text{cyc}} = \alpha_{\text{rich}} - \alpha_{\text{lean}} \quad (9)$$

Here, α_{rich} denotes the CO₂ loading of the initial DEEA solution and α_{lean} denotes the CO₂ loading of the DEEA sample after desorption. Another performance parameter in solvent regeneration experiments is the amount of CO₂ desorbed.^[31] The number of moles of desorbed CO₂ was calculated from the values of CO₂ loading in the liquid phase as shown in Equation (10):

$$n_{\text{CO}_2} = (\alpha_{\text{rich}} - \alpha_{\text{lean}}) \cdot C \cdot V \quad (10)$$

The rate of CO₂ desorption was defined as the CO₂ transfer rate from the DEEA solvent to the gas phase. It was calculated using Equation (11):

$$R_{\text{CO}_2} = \frac{(\alpha_{\text{rich}} - \alpha_{\text{lean}})}{t} \quad (11)$$

The desorption efficiency is another parameter for studying the desorption characteristics. Desorption efficiency was calculated using Equation (12)^[32]:

$$\eta = \frac{\alpha_{\text{rich}} - \alpha_{\text{lean}}}{\alpha_{\text{rich}}} = \frac{Q_{\text{Cyc}}}{\alpha_{\text{rich}}} \quad (12)$$

Q_{Sen} is the energy required to raise the temperature of the DEEA solution. It is necessary to increase the energy

requirement in order to reach low values of the lean solvent loading and high values of the desorption rate. In order to determine the energy required for heating the solvent, the following mathematical relation was used^[33]:

$$Q_{\text{Sen}} = \frac{C_p \Delta T_t}{Q_{\text{Cyc}} X_{\text{DEEA}} M_{\text{CO}_2}} \quad (13)$$

Here, M_{CO_2} is the molecular weight of CO_2 in g/mol, X_{DEEA} is the mole fraction of DEEA in liquid, C_p is the specific heat capacity in kJ/(mol K), and ΔT_t is the temperature difference between time $t=0$ h at which the experiment starts and $t=3$ h at which it stops. All these can be calculated using the experimental values of the respective parameters.

3.5 | Material characterization

To determine the BET surface area and pore size of the material, N_2 sorption measurements were performed by using a Metrohm BELSORP miniX instrument at 77 K with N_2 as the adsorptive gas. Prior to N_2 sorption measurement, samples were degassed at 493 K for 6 h to remove the moisture in the samples. The pore volume, pore diameter, and surface area of the catalysts bentonite and $\text{Bt}/\text{H}_2\text{SO}_4$ were obtained by using the BET method. The structure of catalysts was studied by using the X-ray powder diffraction (XRD) patterns and analyzed in the range of $2\theta = 0-80^\circ$ on SmartLab Studio II, RIGAKU Corporation. Diffraction data were collected on a D/reX Ultra 250 detector using $\text{Cu K}\alpha$ radiation at 45 kV and 40 mA. The SEM technique was used for studying surface morphology (Quanta 200 SEM, FEI). Using FTIR, the spectra for catalysts were obtained (JASCO FT/IR-6600). The acidic properties of $\text{Bt}/\text{H}_2\text{SO}_4$ were investigated using temperature-programmed NH_3 desorption (Micromeritics AutoChem II).

4 | RESULTS AND DISCUSSION

4.1 | Characterization techniques

The properties of bentonite and $\text{Bt}/\text{H}_2\text{SO}_4$ are summarized in Table 1. It is evident that the acidification process remarkably increased the surface area of the parent bentonite catalyst. The commercially available bentonite showed a BET surface area of $46.5 \text{ m}^2/\text{g}$, which increased to $158.48 \text{ m}^2/\text{g}$ after acid treatment with H_2SO_4 . The cations from the clay structure powder promote porosity and removal of these cations significantly increases the surface area. The enhancement in values of the BET surface area

and pore volume confirms that the activation of bentonite with the acid is effective.^[34]

SEM images of both catalysts bentonite and $\text{Bt}/\text{H}_2\text{SO}_4$ are shown in Figure 2A,B. Differently-sized irregular shapes were visible. The catalysts had a porous structure. Both catalysts had granular and porous textures.

The XRD patterns of bentonite and $\text{Bt}/\text{H}_2\text{SO}_4$ catalysts are shown in Figure 3. The XRD diffraction of bentonite showed a highly intense basal peak at $2\theta = 6.47^\circ$, which corresponds to the basal d-spacing (d_{001}) of about 14.69 \AA . The reflections at 19.83° , 26.64° , 35.94° , and 61.76° revealed a bentonite diffractogram.^[24] A sharp reflection of the peak at $2\theta = 26.76^\circ$ indicated α -quartz (silica), which was more intense after acid activation. This demonstrates the variation in the crystal-line structure of bentonite during acidification. The quantity and structure of the organic species are related to the gradual decline in peak intensities, which results in the dissipation of the constructive X-ray interference.^[35] Moreover, a decrease in the intensity of (d_{001}) reflection (14.69 \AA) by comparing parent and modified bentonite showed that $\text{Bt}/\text{H}_2\text{SO}_4$ form was less crystalline.

FTIR spectra was performed in the $400-4000 \text{ cm}^{-1}$ range to obtain evidence for the intercalation of H^+ ions into the bentonite minerals. Figure 4 shows the FTIR curves for natural and acid-activated bentonite. Due to stretching bands of the OH groups, there is a group of absorption peaks between 3450 and 3630 cm^{-1} . The band at 1640 cm^{-1} also corresponds to the OH deformation of water. The peak intensities of acid activated bentonite are lower than that of parent bentonite and this may be acceptable evidence for acid activation occurring on bentonite.^[36]

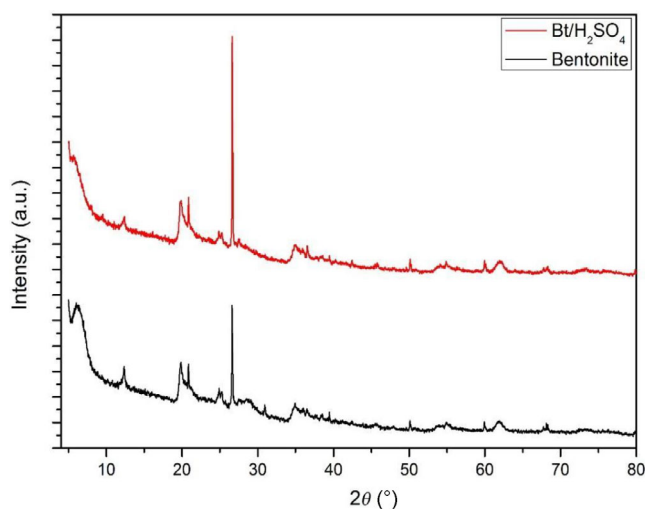
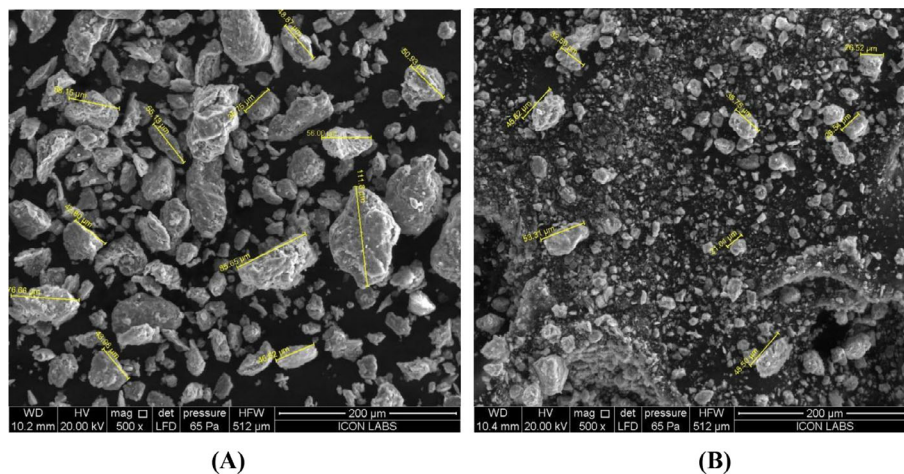
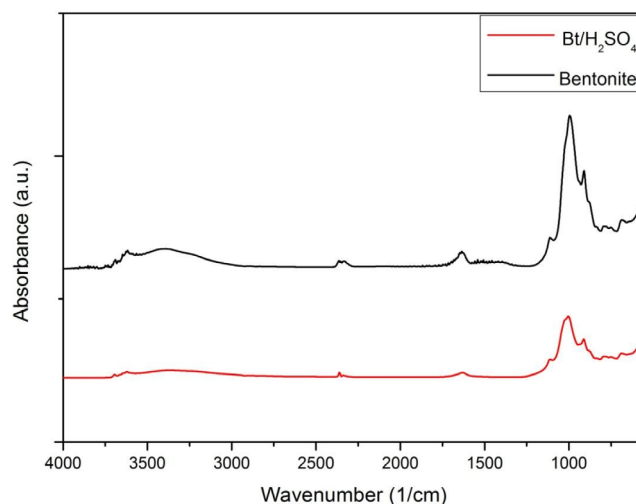
After acid treatment, bentonite catalyst was characterized by NH_3 -TPD tests. The results are shown in Figure 5. The strength of the acidic sites was designated weak or strong based on the temperature region for NH_3 desorption. Peaks at temperatures 458 and 700 K show active acidic sites of 0.035 and 0.057 mmol/g respectively. Furthermore, the peak observed at higher temperatures was broadened, thereby suggesting that the ion-exchange process resulted in the creation of strong acidic sites.

4.2 | Transition metal oxides used for enhanced solvent regeneration

Metal oxides are used extensively as viable solid acid catalysts on a commercial scale. The catalytic behaviour of metal oxides for CO_2 desorption is attributed to their active acidic sites, which are available through surface defects. The acidic sites are of two types: Lewis acid (which can accept a pair of electrons) and Bronsted

TABLE 1 Textural properties of catalysts.

Catalysts	S_{BET} (m^2/g)	V_{pore} (cm^3/g)	Average pore diameter (nm)
Bentonite	46.5	0.0412	3.61
Bt/ H_2SO_4	158.48	0.0994	2.5

FIGURE 2 Scanning electron microscope images of (A) bentonite and (B) Bt/ H_2SO_4 .**FIGURE 3** X-ray diffraction (XRD) patterns of the bentonite and Bt/ H_2SO_4 .**FIGURE 4** Fourier transform infrared spectrometry (FTIR) spectra curves of bentonite and acid activated bentonite Bt/ H_2SO_4 .

acid sites (which can donate a hydrogen cation). Idem et al.^[37] introduced $\gamma\text{-Al}_2\text{O}_3$ as a preferable solid acid catalyst for CO_2 stripping. They reported that the addition of $\gamma\text{-Al}_2\text{O}_3$ to aqueous 5 M MEA solution can decrease the regeneration temperature from 393–413 to 363–368 K and regeneration energy by 27%. Due to the commercial availability of $\gamma\text{-Al}_2\text{O}_3$, it became a benchmark for further investigation.

In the present work, 0.12 mol of CO_2 were desorbed from 2.5 M DEEA at $T = 363$ K. Under the same experimental conditions, catalyst addition enhances CO_2 desorption performance and accelerates amine regeneration compared to a non-catalytic system. The cyclic

capacity of 2.5 M DEEA solution was estimated using 10 different catalysts at 363 K. The lean CO_2 loadings were recorded for both catalytic and non-catalytic solutions of DEEA. Compared to non-catalytic solvents, catalytic solvents can achieve higher cyclic capacities, as shown in Figure 6A.

Higher desorption efficiency and lower regeneration energy are additional effects of increased cyclic capacity. The major reason for the observed increase in cyclic capacity is the presence of more acidic sites, which are effective in carbamate protonation. Apart from the cyclic capacities, the amount of CO_2 desorbed, the CO_2 desorption efficiency and the rate of CO_2 desorption were

evaluated. These values for catalytic solvents were higher than those for non-catalytic solvents. The estimated values of these parameters are represented in Table 2. The increase in percentage CO₂ desorption efficiency is shown in Figure 6B.

The improvement in desorption performance for catalytic DEEA system was investigated. It was observed that among all transition metal oxides, γ -Al₂O₃ (89.3%) exhibited the highest desorption efficiency, followed by MoO₃ (87.6%), V₂O₅ (68.3%), TiO₂ (66.3%), MnO₂ (63.7%), ZnO (62.1%), Cr₂O₃ (58.6%), SiO₂ (53.8%), and ZrO₂ (52.3%). Other than these nine transition metal oxides, one cheap and abundantly available clay-based material bentonite

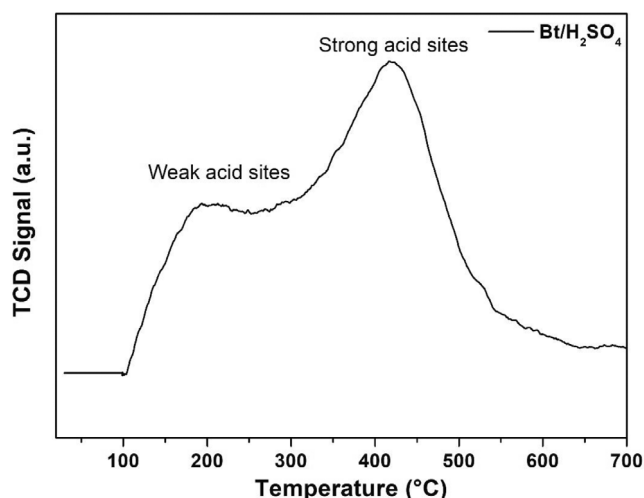


FIGURE 5 The results of ammonia temperature-programmed desorption (NH₃-TPD) test for Bt/H₂SO₄ catalyst. TCD, thermal conductivity detector.

was also used as catalyst for regeneration of amine solvent. The efficiency of desorption for the DEEA-Bt system was recorded as 64.9%, which is comparable to the results obtained using the metal oxides in this work.

4.3 | Effect of acid-activated bentonite on solvent regeneration

The addition of acidic catalyst to the regeneration system provides free electrons from both Bronsted acid and Lewis acid sites. These sites readily bind to the carbamate and facilitate zwitterion formation. The N—C bond is weakened, thereby resulting in reduced energy requirement. Additionally, catalysts provide protons to carbonate and bicarbonate ions, thus resulting in the formation of carbonic acid and easing the subsequent release of CO₂.^[34]

Sulphurization of a catalyst has shown improved effects on the Lewis and Bronsted acidity of metal oxide catalysts, due to the interaction between metals and sulphates caused by the strong electron withdrawing effect of the S=O double bonds.^[38] The original bentonite was acidified with four acids separately and the solvent regeneration parameters were calculated and presented in Table 3.

In comparison to DEEA-Bt, which showed a desorption rate of 6.54×10^{-2} mol of CO₂/(mol of DEEA-h) and sensible energy of 22 MJ/kg of CO₂ at 363 K, DEEA-Blank samples exhibited desorption rate of 4×10^{-2} mol of CO₂/(mol of DEEA-h) and sensible energy of 35.9 MJ/kg of CO₂ at 363 K. This demonstrates the reduction in sensible energy. The cyclic capacity of acid-activated bentonite is shown in

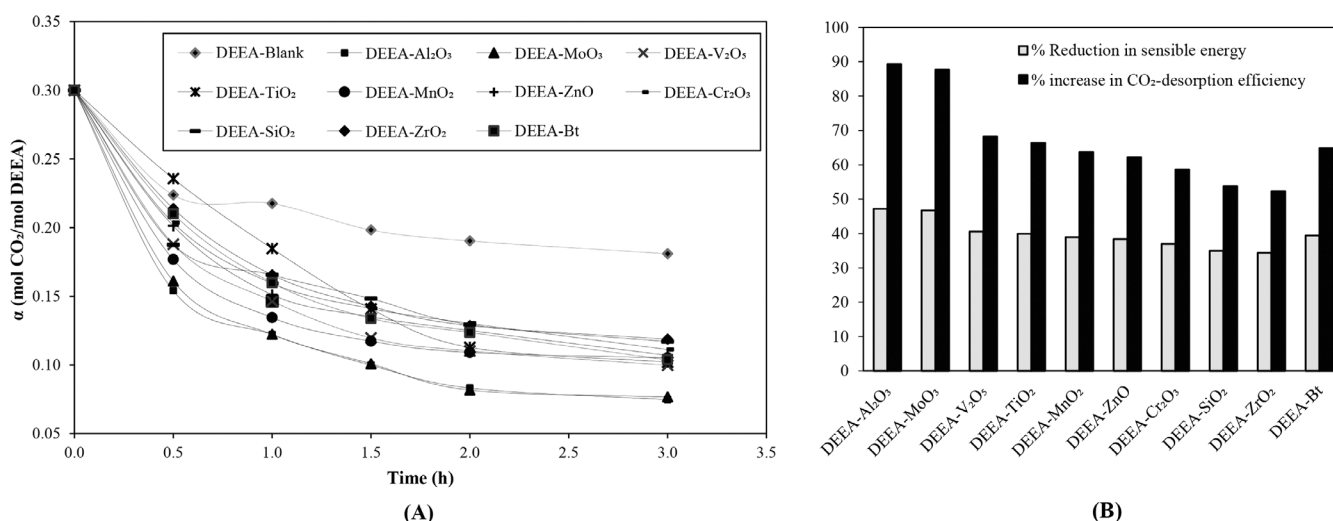


FIGURE 6 Desorption performance of various transition metal oxide catalysts for 2.5 M N,N'-diethylethanolamine (DEEA) at $T = 363$ K: (A) CO₂ loading versus time and (B) % reduction in sensible energy and % increase in CO₂-desorption efficiency.

TABLE 2 CO₂-desorption performance of 2.5 M N,N'-diethylethanolamine (DEEA) with and without catalysts at $T = 368$ K.

DEEA-catalyst systems	α_{rich} (mol of CO ₂ /mol of DEEA)	α_{lean} (mol of CO ₂ /mol of DEEA)	Q_{cyc} (mol of CO ₂ /mol of DEEA)	n_{CO_2} (mol of CO ₂ desorbed)	Γ (mol)	R_{CO_2} (mol of CO ₂ /(mol of DEEA-h))	Q_{Sen} (MJ/kg of CO ₂)
DEEA-Blank	0.32	0.18	0.12	0.119	0.397	3.97	0
DEEA-Al ₂ O ₃	0.32	0.07	0.23	0.225	0.751	7.51	47.17
DEEA-MoO ₃	0.32	0.08	0.22	0.223	0.745	7.45	46.70
DEEA-V ₂ O ₅	0.34	0.10	0.20	0.200	0.668	6.68	40.57
DEEA-TiO ₂	0.3	0.10	0.20	0.198	0.660	6.6	39.88
DEEA-MnO ₂	0.32	0.11	0.19	0.195	0.650	6.5	38.91
DEEA-ZnO	0.32	0.11	0.19	0.193	0.643	6.43	38.32
DEEA-Cr ₂ O ₃	0.32	0.11	0.19	0.189	0.629	6.29	36.95
DEEA-SiO ₂	0.31	0.12	0.18	0.183	0.610	6.1	34.96
DEEA-ZrO ₂	0.33	0.12	0.18	0.181	0.604	6.04	34.33
DEEA-Bt	0.32	0.10	0.20	0.196	0.654	6.54	39.35

TABLE 3 CO₂-desorption performance of bentonite catalyst in 2.5 M N,N'-diethylethanolamine (DEEA) with and without acid treatment at $T = 368$ K.

DEEA-catalyst systems	α_{rich} (mol of CO ₂ /mol of DEEA)	α_{lean} (mol of CO ₂ /mol of DEEA)	Q_{cyc} (mol of CO ₂ /mol of DEEA)	n_{CO_2} (mol of CO ₂ desorbed)	Γ (mol)	R_{CO_2} (mol of CO ₂ /(mol of DEEA-h))	Q_{Sen} (MJ/kg of CO ₂)
Bentonite	0.32	0.10	0.20	0.196	0.654	65.4	39.35
Bt/HCl	0.3	0.09	0.21	0.210	0.701	70.1	43.37
Bt/H ₃ PO ₄	0.32	0.08	0.22	0.219	0.731	73.1	45.69
Bt/HNO ₃	0.31	0.06	0.24	0.230	0.767	76.7	48.24
Bt/H ₂ SO ₄	0.3	0.07	0.23	0.239	0.796	79.6	50.17

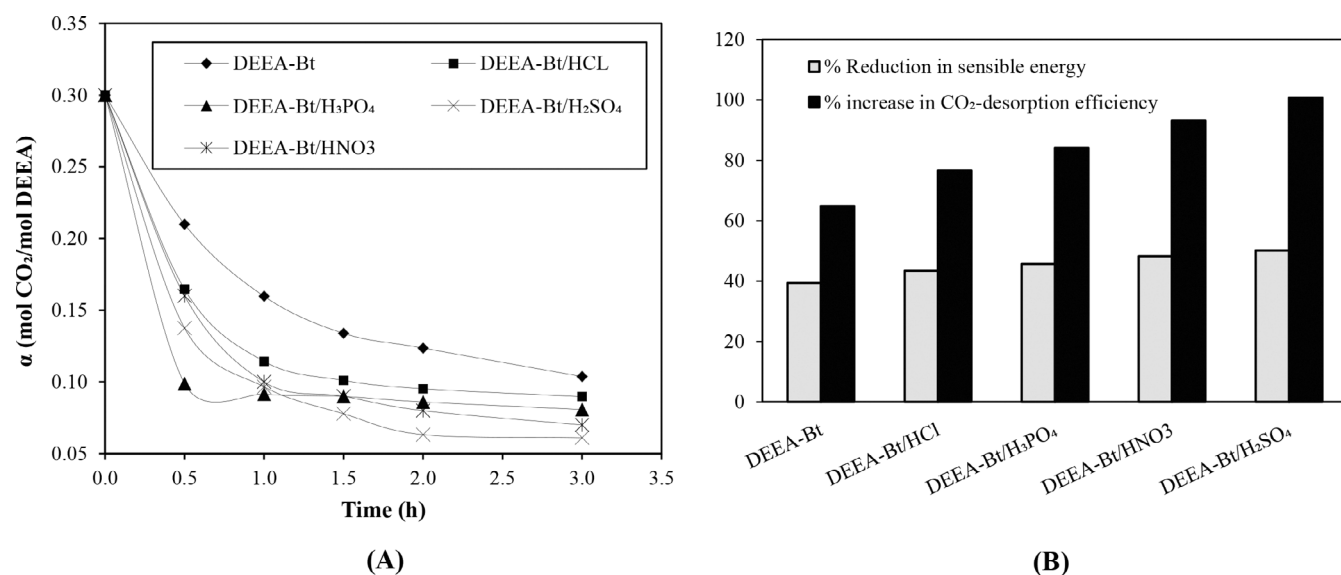
FIGURE 7 Desorption performance of four acidified bentonite catalysts in 2.5 M N,N'-diethylethanolamine (DEEA) at $T = 363$ K: (A) CO₂ loading versus time and (B) % reduction in sensible energy and % increase in CO₂-desorption efficiency.

Figure 7A. The desorption efficiency of Bt/H₂SO₄ (100.7%) was found to be the highest compared with other samples of bentonite acidified using HCl (76.6%), H₃PO₄ (84.1%), and HNO₃ (93.2%). The results are shown in Figure 7B. This is attributed to the improved surface area (see Table 1) and active acidic sites (see Figure 5) in Bt/H₂SO₄. Tan et al.^[13] proved that activated clay ATP was durable and could be recycled 15 times without any adverse fall in its activity. Bhatti et al.^[33] earlier reported that montmorillonite clay activated with H₂SO₄ was stable for five absorption–regeneration cycles. Thus, we anticipated that the cyclic stability of Bt/H₂SO₄ would be encouraging. This is the topic of our forthcoming study on clay-assisted amine desorption.

MEA is the baseline solution for the amine-based CO₂ capture technology. Thus, the performance of acid-modified bentonite catalyst in the desorption of CO₂-rich MEA solutions was studied. Trials performed using 2.5 MEA solutions at 363 K suggested that the desorption rates for bentonite and Bt/H₂SO₄ were 3.47×10^{-2} and 4.64×10^{-2} mol of CO₂/(mol of MEA-h). The respective values of desorption efficiency were 31% and 38%. The efficacy of the chosen catalysts for desorption of rich MEA solutions was thus evident.

5 | CONCLUSIONS

In summary, adding catalyst significantly accelerates the CO₂ desorption mechanism and decreases energy consumption. In this work, catalysts helped to reduce energy requirements for the regeneration process of DEEA by enhancing the rate of CO₂ desorption. The performance of metal oxide catalysts was evaluated and found to be in hierarchy of γ -Al₂O₃ (89.3%), MoO₃ (87.6%), V₂O₅ (68.3%), TiO₂ (66.3%), MnO₂ (63.7%), ZnO (62.1%), Cr₂O₃ (58.6%), SiO₂ (53.8%), and ZrO₂ (52.3%). One clay-based material bentonite was introduced as a catalyst in this work and it showed desorption efficiency (64.9) comparable with the reported metal oxides. Due to its low cost and easy availability, bentonite powder was further treated with acids (HCl, H₃PO₄, HNO₃, and H₂SO₄) to improve the catalytic characteristics and desorption rate of CO₂. Among these four acidified samples, Bt/H₂SO₄ recorded highest desorption rate (7.96×10^{-2} mol of CO₂/[mol of DEEA-h]). Moreover, the characterization of Bt/H₂SO₄ indicated increased surface area and pore volume compared to the parent bentonite. Based on these results, bentonite powder can be recommended as a catalyst for the CO₂ desorption process for DEEA solvent and acid-activation can be considered if the performance of original bentonite needs to be enhanced.

NOMENCLATURE

C	concentration of DEEA solution (mol/L)
(CO_2)	concentration of CO ₂ in the liquid phase (mol/L)
C_p	specific heat capacity (kJ/mol-K)
$k_{\text{R}_3\text{N}}$	reaction rate constant in equation 7
M_{CO_2}	molecular weight of CO ₂ (g/mol)
n_{amine}	moles of amine (mol)
n_{CO_2}	moles of CO ₂ (mol)
Q_{cyc}	cyclic capacity (mol CO ₂ /mol DEEA)
Q_{Sen}	sensible heat (MJ/kg of CO ₂)
r_{CO_2}	rate of reaction between CO ₂ and R ₃ N
R_{CO_2}	CO ₂ desorption rate (mol CO ₂ /mol DEEA-h)
(R_3N)	concentration of the tertiary amine R ₃ N in the liquid phase (mol/L)
S_{BET}	BET surface area (m ² /g)
t	time (h)
T	temperature (K)
ΔT_t	temperature difference (K)
V	volume of DEEA solution (L)
V_{pore}	pore volume (cm ³ /g)
X_{DEEA}	mole fraction of DEEA

Greek symbols

\propto	loading capacity of CO ₂ (mol CO ₂ /mol DEEA)
\propto_{rich}	rich loading capacity of CO ₂ (mol CO ₂ /mol DEEA)
\propto_{lean}	lean loading capacity of CO ₂ (mol CO ₂ /mol DEEA)
η	desorption efficiency

AUTHOR CONTRIBUTIONS

Urvashi K. Sarode: Investigation; methodology; validation; writing – original draft. **Prakash D. Vaidya:** Conceptualization; funding acquisition; supervision; writing – review and editing.

ACKNOWLEDGEMENTS

Urvashi Kishor Sarode is thankful to the Department of Science and Technology, Ministry of Science and Technology, Government of India, New Delhi, for providing financial assistance [Grant/award number: DST/TM/EWO/MI/CCUS/11(G) dated September 2019].


PEER REVIEW

The peer review history for this article is available at <https://www.webofscience.com/api/gateway/wos/peer-review/10.1002/cjce.25105>.

DATA AVAILABILITY STATEMENT

The data that support the findings of this study are available from the corresponding author upon reasonable request.

ORCID

Prakash D. Vaidya  <https://orcid.org/0000-0001-5061-9635>

REFERENCES

- [1] P. D. Vaidya, E. Y. Kenig, *Ind. Eng. Chem. Res.* **2008**, 47, 34.
- [2] J. T. Yeh, H. W. Pennline, K. P. Resnik, *Energy Fuels* **2001**, 15, 274.
- [3] E. Joseph, P. D. Vaidya, *Int. J. Chem. Kinet.* **2019**, 51, 31.
- [4] P. D. Vaidya, E. Y. Kenig, *Chem. Eng. Sci.* **2007**, 62, 7344.
- [5] P. N. Sutar, P. D. Vaidya, E. Y. Kenig, *Chem. Eng. Sci.* **2013**, 100, 234.
- [6] F. A. Chowdhury, H. Yamada, T. Higashii, K. Goto, *Ind. Eng. Chem. Res.* **2013**, 52, 8323.
- [7] U. H. Bhatti, A. K. Shah, J. N. Kim, J. K. You, S. H. Choi, D. H. Lim, S. Nam, Y. H. Park, I. H. Baek, *ACS Sustainable Chem. Eng.* **2017**, 5, 5862.
- [8] U. H. Bhatti, S. Nam, Y. H. Park, I. H. Baek, *ACS Sustainable Chem. Eng.* **2018**, 6, 12079.
- [9] U. H. Bhatti, D. Sivanesan, D. H. Lim, S. C. Nam, S. Y. Park, I. H. Baek, *J. Taiwan Inst. Chem. Eng.* **2018**, 93, 150.
- [10] X. Zhang, Z. Zhu, X. Sun, J. Yang, H. Gao, Y. Huang, X. Luo, Z. Liang, P. Tontiwachwuthikul, *Environ. Sci. Technol.* **2019**, 53, 6094.
- [11] X. Zhang, Y. Huang, J. Yang, H. Gao, Y. Huang, X. Luo, Z. Liang, P. Tontiwachwuthikul, *Chem. Eng. J.* **2019**, 383, 123077.
- [12] R. Zhang, T. Li, Y. Zhang, J. Ha, Y. Xiao, C. Li, X. Zhang, H. Luo, *Sep. Purif. Technol.* **2022**, 300, 121702.
- [13] Z. Tan, S. Zhang, X. Yue, F. Zhao, F. Xi, D. Yan, H. Ling, R. Zhang, F. Tang, K. You, H. Luo, X. Zhang, *Sep. Purif. Technol.* **2022**, 298, 121577.
- [14] Z. Tan, S. Zhang, F. Zhao, R. Zhang, F. Tang, K. You, H. Luo, X. Zhang, *Chem. Eng. J.* **2023**, 453, 139801.
- [15] R. E. Grim, N. Guven, *Bentonite—Geology, Mineralogy, Properties and Uses, Development in Sedimentology*, Vol. 24, Elsevier, Amsterdam, the Netherlands **1978**.
- [16] R. E. Grim, *Clay Mineralogy*, McGraw-Hill, New York **1968**.
- [17] H. H. Murray, *Appl. Clay Sci.* **1991**, 5, 379.
- [18] M. Onal, Y. Sarikaya, *Powder Technol.* **2007**, 172, 14.
- [19] V. A. Arus, S. Nousir, R. Sennour, T. C. Shiao, I. D. Nistor, R. Roy, A. Azzouz, *Int. J. Hydrogen Energy* **2018**, 43, 7964.
- [20] X. Zhang, J. Hong, H. Liu, X. Luo, W. Olson, P. Tontiwachwuthikul, Z. Liang, *AIChE J.* **2018**, 64, 3988.
- [21] M. S. Alivand, O. Mazaheri, Y. Wu, G. W. Stevens, C. A. Scholes, K. A. Mumford, *ACS Sustainable Chem. Eng.* **2020**, 8, 18755.
- [22] H. Liu, M. Xiao, P. Tontiwachwuthikul, Z. Liang, *Energy Procedia* **2017**, 105, 4476.
- [23] M. Caplow, *J. Am. Chem. Soc.* **1968**, 90, 6795.
- [24] P. V. Danckwerts, *Chem. Eng. Sci.* **1979**, 34, 443.
- [25] P. D. Vaidya, E. Y. Kenig, *Chem. Eng. Technol.* **2010**, 30, 1577.
- [26] P. D. Vaidya, E. Y. Kenig, *Chem. Eng. Technol.* **2007**, 30, 1467.
- [27] T. L. Donaldson, N. Y. Nguyen, *Ind. Eng. Chem. Fundam.* **1980**, 19, 260.
- [28] G. Altabash, M. Al-Hindi, F. Azizi, *Ind. Eng. Chem. Res.* **2020**, 59, 11691.
- [29] Z. Liang, R. Idem, P. Tontiwachwuthikul, F. Yu, H. Liu, W. Rongwong, *AIChE J.* **2016**, 62, 753.
- [30] N. Horri, E. S. Sanz-Perez, A. Arencibia, R. Sanz, N. Frini-Srasra, E. Srasra, *Appl. Clay Sci.* **2019**, 180, 105195.
- [31] S. H. Joo, U. H. Bhatti, H. J. Park, D. H. Jeong, I. H. Baek, S. C. Nam, K. B. Lee, *Chem. Eng. Process.* **2020**, 147, 107772.
- [32] C. Dinca, A. Badea, *Int. J. Greenhouse Gas Control* **2013**, 12, 269.
- [33] U. H. Bhatti, H. Sultan, G. H. Min, S. C. Nam, I. H. Baek, *Chem. Eng. J.* **2021**, 413, 127476.
- [34] U. H. Bhatti, W. W. Kazmi, H. A. Muhammad, H. Sultan, G. H. Min, S. C. Nam, I. H. Baek, *Green Chem.* **2020**, 22, 6328.
- [35] G. Calleja, R. Sanz, A. Arencibia, E. S. Sanz-Perez, *Top. Catal.* **2011**, 54, 135.
- [36] A. Salem, L. Karimi, *Korean J. Chem. Eng.* **2009**, 26, 980.
- [37] R. Idem, H. Shi, D. Gelowitz, P. Tontiwachwuthikul, *WO2011120138A1*. **2011**.
- [38] H. Wang, Z. Qu, S. Dong, C. Tang, *ACS Appl. Mater. Interfaces* **2017**, 9, 7017.

How to cite this article: U. K. Sarode, P. D. Vaidya, *Can. J. Chem. Eng.* **2024**, 102(3), 1262.
<https://doi.org/10.1002/cjce.25105>